

# Intricate routes to chaos in the Mackey–Glass delayed feedback system

Leandro Junges<sup>a,b</sup>, Jason A.C. Gallas<sup>a,b,c,\*</sup>

<sup>a</sup> Institute for Multiscale Simulation, Friedrich-Alexander Universität, Nögelsbachstraße 49b, 91052 Erlangen, Germany

<sup>b</sup> Instituto de Física, Universidade Federal do Rio Grande do Sul, 91501-970 Porto Alegre, Brazil

<sup>c</sup> Departamento de Física, Universidade Federal da Paraíba, 58051-970 João Pessoa, Brazil

## ARTICLE INFO

### Article history:

Received 28 March 2012

Received in revised form 27 April 2012

Accepted 9 May 2012

Available online 14 May 2012

Communicated by A.R. Bishop

### Keywords:

Mackey–Glass equation

Feedback systems

Delay-differential equations

Numerical simulations of chaotic systems

## ABSTRACT

We describe some remarkable *continuous deformations* which create and destroy peaks in periodic oscillations of the Mackey–Glass equation, a paradigmatic example of a delayed feedback system. Peak creation and destruction results in richer bifurcation diagrams which, in addition to the familiar branches arising from period-doubling and peak-adding bifurcations, may also display arbitrary combinations of doubling and adding, leading to highly complex mosaics of stability domains in control parameter space. In addition, we show that the onset of higher dimensionality does not alter the prevailing dynamics *instantaneously* and, remarkably, even may have no effect at all, a result that cannot be predicted analytically with standard methods.

© 2012 Elsevier B.V. All rights reserved.

## 1. Introduction

The aim of this Letter is to report some intricate routes to chaos observed in the Mackey–Glass (MG) equation, a paradigmatic delayed feedback system introduced to model oscillations and chaos present in a control physiological system related to dynamical respiratory and hematopoietic diseases [1–3]. Presently, delayed feedback systems are an active area of research across different disciplines of science and technology like, e.g. in innovative applications involving semiconductor lasers [4,5]. Such feedback processes are also central to life, governing how we grow, respond to stress and challenge, and regulating factors such as body temperature, blood pressure and cholesterol level. Delayed feedback mechanisms operate at every level, from the interaction of proteins in cells to the interaction of organisms in complex ecologies [6,7].

Mathematically, delayed feedback systems are described by delay-differential equations (DDEs), equations far more complex than ordinary differential equations (ODEs), implying that the properties of DDEs are far less understood than for ODEs. For simplicity, here we focus on phenomena which we observed in the *single-variable* Mackey–Glass equation. We mention, however, that analogous phenomena are also present in *multi-variables* delayed feedback systems such as semiconductor lasers [8].

The intricate routes to chaos described below arise from remarkable *continuous deformations* responsible for creating and destroying isolated peaks in periodic oscillations of the MG equation. The creation and destruction of single peaks in oscillatory patterns have the net effect of producing richer bifurcation diagrams which, as described below, may display *arbitrary combinations* of period-doubling and peak-adding bifurcations. The result of such combinations is to produce highly complex mosaics of stability domains in control parameter space, as exemplified in the phase diagrams presented below.

Before proceeding, recall that even just a *single* delay-differential equation is already equivalent to an *infinite* dimensional ODE system [9–12]. This means that delayed feedback systems are far more complicated than systems governed by ODEs. Accordingly, there are much less analytical results and methods for DDEs than for ODEs. For instance, analytical results for DDEs do not go beyond fix-point analysis which are usually based on approximations of some sort like, e.g. asymptotic expansions. DDEs are computationally intense systems to digest, a fact that helps to explain why so far they were much less investigated.

Here we present novel phenomena observed during a systematic numerical investigation of the MG equations. Our presentation is essentially descriptive due to the complicated nature of the DDEs and, as mentioned, to the absence of general methods to go beyond fix-point analysis into the new unexplored realm of solutions with *arbitrary periodicities* and chaos. As will become clear, our results uncover a number of regularities and tendencies worth pursuing analytically.

As an interesting additional byproduct, we show that the onset of the infinite dimensionality characteristic of DDEs does not

\* Corresponding author at: Instituto de Física, Universidade Federal do Rio Grande do Sul, 91501-970 Porto Alegre, Brazil. Tel.: +55 51 3308 6522; fax: +55 51 3308 7286.

E-mail address: jgallas@if.ufrgs.br (J.A.C. Gallas).

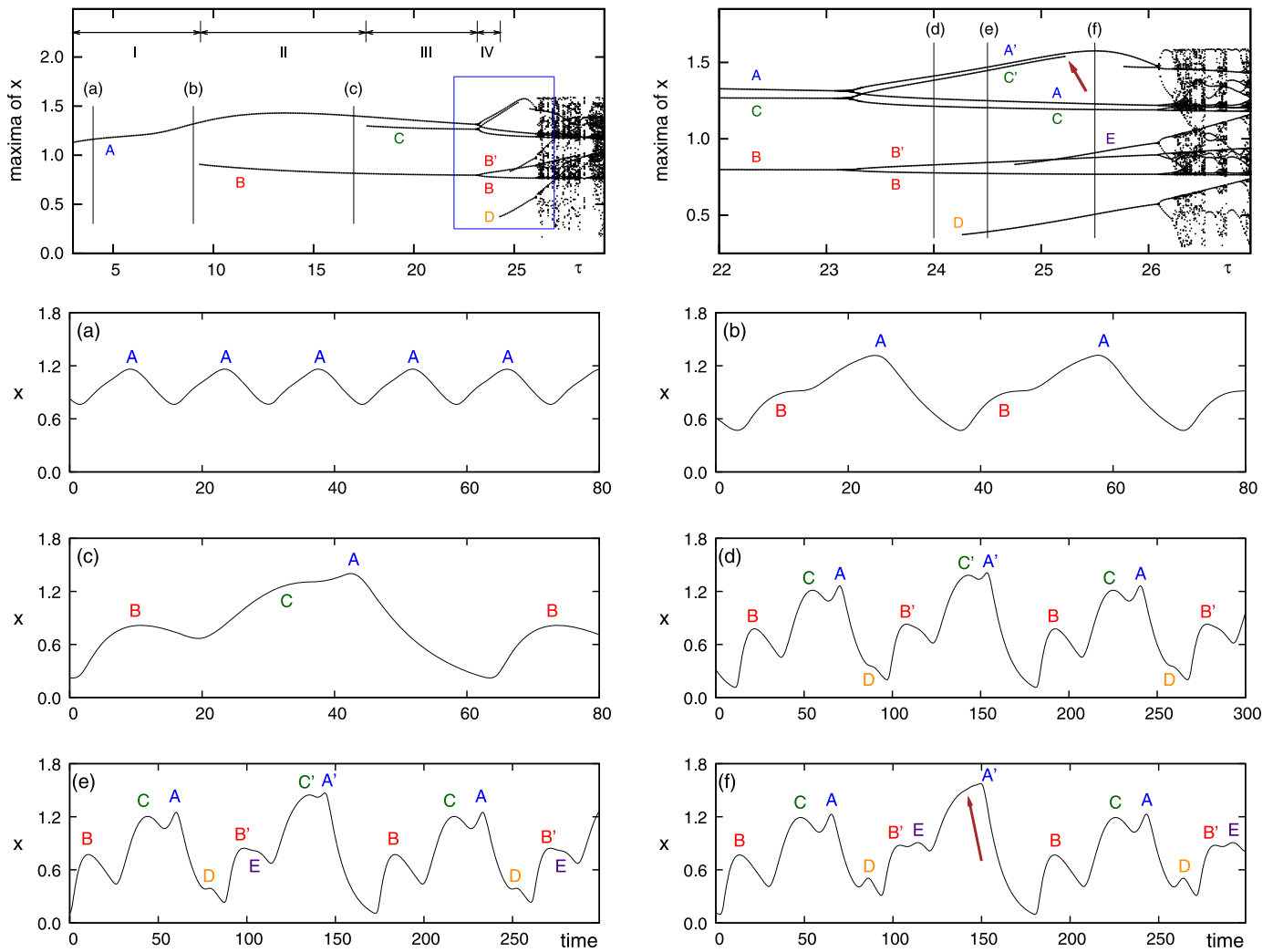


**Fig. 1.** (Color online.) The route to chaos via waveform deformation observed generically in delayed feedback systems. The top line shows bifurcation diagrams for Eq. (1) with  $n = 21$  (the white horizontal line in Fig. 4 below). The other panels show the time evolution of the oscillations for selected values of the delay  $\tau$ . (a)  $\tau = 4$ , oscillation with a single peak, of amplitude A; (b)  $\tau = 9$ , precursor of peak B is visible; (c)  $\tau = 17$ , oscillation with two peaks, A and B, and precursor of C; (d)  $\tau = 24$ , period-doublings (A, A'), (B, B') and (C, C'); precursor of D is visible; (e)  $\tau = 24.5$ , precursor of E is visible; (f)  $\tau = 25.5$ , sudden death of peak C', indicated by the arrow.

alter the prevailing dynamics *instantaneously*, and even may have no effect at all. This remarkable result cannot be obtained using standard techniques commonly used to analyze DDEs like, e.g. perturbation theory [9–12].

**2. Continuous waveform deformations and isolated branches**

The Mackey–Glass model is defined by the single-variable equation [1–3]

$$\frac{dx}{dt} = f(x, x_\tau) \equiv \frac{\beta x_\tau}{1 + (x_\tau)^n} - \gamma x, \tag{1}$$

where  $x_\tau \equiv x(t - \tau)$  represents the variable  $x$  at time  $t - \tau$ , and  $\beta, \gamma, \tau, n > 0$  are real parameters. Depending on the parameters, this equation is known to display a range of periodic and chaotic dynamics [2,3]. Following tradition, we focus on the original Mackey–Glass parameters, namely,  $\beta = 0.2$  and  $\gamma = 0.1$ . Results for them are generic. For completeness, we mention that a bifurcation analysis of the Mackey–Glass equation is already available, in particular that a sequence of Hopf bifurcations occurs at the equilibrium as the delay increases [13,14].

The top row of Fig. 1 displays typical bifurcation diagrams obtained by plotting the maxima, peaks, of the numerically computed

solutions as a function of  $\tau$ . In these diagrams it is possible to recognize the presence of the familiar period-doubling branches. However, very distinctly from bifurcation diagrams known for maps and flows, these figures also show that bifurcation diagrams for delay-differential equations may also contain *isolated branches*, namely single branches that begin or end quite abruptly for specific parameter values. Examples of isolated branches beginning suddenly are the ones labeled B, C and D in the left panel at the top of Fig. 1. An example of a branch ending abruptly is the branch C', indicated by the arrow in the right panel at the top. It is natural to ask about the origin of such discontinuities. To understand them, we study the time evolution of the solutions before and after the discontinuities, for the values of  $\tau$  indicated by the vertical line segments (a), (b), ..., (f) in the pair of panels at the top row of Fig. 1.

Fig. 1(a) shows the time-evolution of  $x(t)$  for  $\tau = 4$ , namely for a value far from the beginning of branch B. As illustrated by Fig. 1(a), in this case  $x(t)$  is characterized by a smooth periodic oscillation with a single peak A within the period. For  $\tau = 9$ , just before the beginning of B, the oscillation remains periodic but starts to develop an inflexion point B as indicated in Fig. 1(b). We write B below the curve to indicate the fact that this point is not yet a local maximum of the curve: it is simply a “precursor”

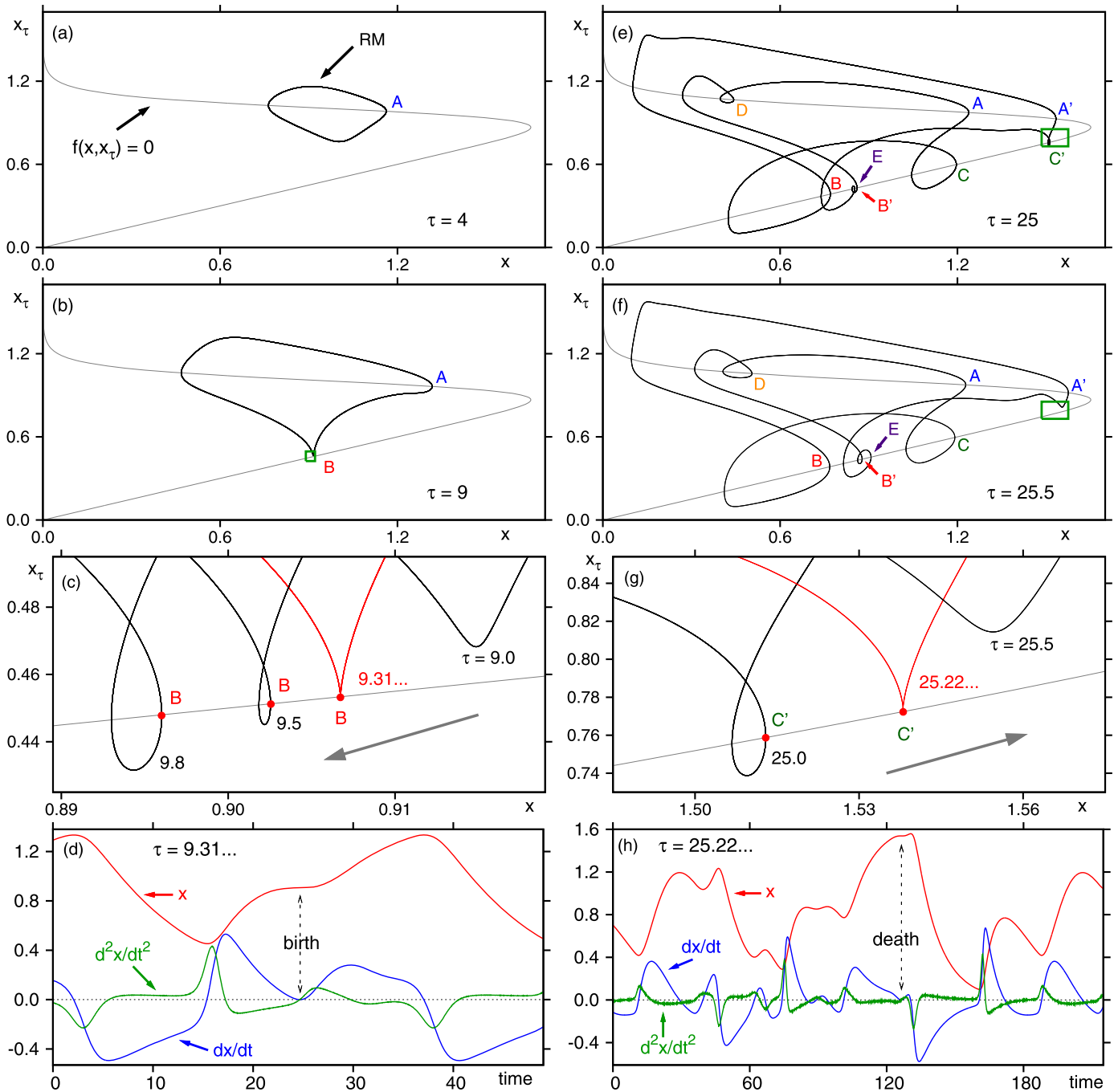


**Fig. 2.** (Color online.) Return maps (RM) illustrating the birth and death of the isolated branches seen in bifurcation diagrams in Fig. 1. The left column shows the birth of branch B while in the right column we depict how branch C' disappears. Panels (a)–(c) and (e)–(f) show the formation of a cusp when the return map meets the curve  $f(x, x_\tau) = 0$ , as indicated in (c) and (g). The three curves in panels (d) and (h) display the time evolution of  $x$ ,  $dx/dt$ , and  $d^2x/dt^2$ . As indicated by the dashed arrows, cusps occur whenever  $dx/dt = d^2x/dt^2 = 0$ . Here  $n = 21$ . See the text for a detailed description.

of what will become a real local maximum when increasing  $\tau$ , giving then birth to the branch B. In Fig. 1(c) we illustrate a situation where B is a local maximum of the solution (which now displays two peaks within a period). Similarly as before, the point C under the curve indicates the precursor of branch C. Fig. 1(d) illustrates the time-evolution for  $\tau = 17$  (vertical segment (d) in the right panel of the top row). In this figure we easily recognize the period-doubled peak pairs of similar amplitude, namely (A, A'), (B, B'), and (C, C'). Also indicated in Fig. 1(d) is the position of the precursor of peak D. Similarly, Fig. 1(e) shows peak D and the precursor of E. From this unfolding, one realizes the reason behind

the emergence of the “extra” branches in the bifurcation diagrams: they all result from deformations suffered by the waveform of the solution as the parameter varies.

How do branches suddenly disappear from bifurcation diagrams? This may be understood by comparing the point indicated by the arrow in Fig. 1(f) with point C' in Fig. 1(e). This comparison shows that peak C' is destroyed by a deformation inverse to the one responsible for the sudden creation of branches. We observed such creations to occur profusely in the Mackey–Glass equation. Thus, we believe these pattern deformations inducing creation and destruction of peaks to be a generic characteristic of

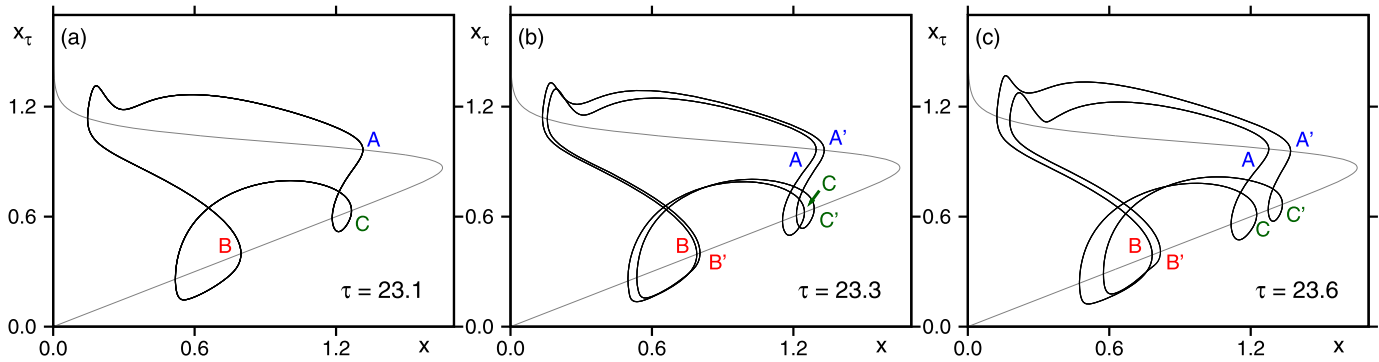


**Fig. 3.** (Color online.) Unfolding of a period-doubling (A, A'), (B, B') and (C, C') which happens for values of  $\tau$  between those of Figs. 1(c) and (d). The doubling occurs near  $\tau \simeq 23.2$ . In (c), one can see imminence of the cuspidal intersection that will give rise to the isolated branch D described in Fig. 1. Here  $n = 21$ .

delay-differential equations, not just a peculiarity of the illustrative model considered.

The extra isolated branches arising through the waveform deformations described above should not be confused with the very common discontinuous branches which arise in bifurcation diagrams due to multistability. The latter involve *distinct basins of attraction* while in the former the attractor evolves continuously staying always inside *the same basin of attraction*. Isolated branches can be recognized in bifurcation diagrams reported previously in the literature of delayed feedback systems, e.g. in Ref. [15] for the Mackey–Glass equation. However, we have not found any earlier reference addressing them. Although we have also not been able to locate references discussing waveform deformations and isolated branches occurring in ODEs, we see no reason for such deformations not to exist in them.

### 3. Return maps and genesis of isolated branches

As explained in the previous section, the signature of the birth and death of isolated branches in the bifurcation diagrams is the occurrence of inflexion points in the waveforms as parameters are tuned. Inflexion points occur when both the first and the second derivatives are zero (the second derivative changes sign):

$$\frac{dx}{dt} = \frac{d^2x}{dt^2} = 0, \quad \text{and} \quad \frac{d^3x}{dt^3} \neq 0. \quad (2)$$

The detailed genesis of isolated branches in bifurcation diagrams can be understood by investigating how the return map (RM)  $x(t) \times x(t - \tau)$  evolves as a function of  $\tau$ . Fig. 2 shows several examples of such return maps plotted together with the solution of  $f(x, x_\tau) = 0$ , where  $f(x, x_\tau)$  is the function defined in Eq. (1).

Fig. 2(a) illustrates this pair of curves for  $\tau = 4$ . The return map (indicated by the letters RM) is the thicker curve, a closed loop which intersects the lighter trace, solutions of  $f(x, x_\tau) = 0$ , in two locations: a minimum (on the left) and a maximum, indicated by A. The point A is the same one marked in the bifurcation diagrams in Fig. 1 and below them, in Fig. 1(a). As  $\tau$  increases, the loop grows and gets deformed continuously, developing a region of strong curvature near the point labeled B in Fig. 1(b). Next, in Fig. 1(c), we summarize what happens when further increasing  $\tau$ : the return map crosses once again the curve  $f(x, x_\tau) = 0$ . For  $\tau_{\text{birth}} = 9.31 \dots$  the return map shows a cusp that meets the solution of  $f(x, x_\tau) = 0$ . Upon further increase of  $\tau$ , the cusp develops a loop, as illustrated for  $\tau = 9.5$  and  $9.8$ . The arrow in this figure indicates the direction of displacement of the return maps as  $\tau$  increases. Fig. 2(d) displays the time evolutions of  $x$ ,  $dx/dt$ , and  $d^2x/dt^2$ , where the dashed arrow marks the birth of the isolated branch B in the bifurcation diagram.

By further increasing  $\tau$  the return map develops additional loops and intersection, as illustrated in Figs. 2(e) and 2(f). These intermediary panels help to understand the unfolding of the bifurcations seen in Fig. 1 and, more importantly, to understand how isolated branches die. As indicated by the arrow in Fig. 2(g), when  $\tau$  increases one sees that the death of the isolated branch C' occurs by an inverse process of that responsible for creating isolated branches and depicted in Fig. 2(c): An existing loop collapses to a cusp for  $\tau_{\text{death}} = 25.22 \dots$ , the point where upon further increase of  $\tau$  the intersection disappears. The corresponding time evolutions of  $x$ ,  $dx/dt$ , and  $d^2x/dt^2$  are shown in Fig. 2(h).

To conclude this section, Fig. 3 illustrates how a period-doubling unfolds as  $\tau$  increases. In the case in hand one sees the bifurcation of the peaks A, B and C seen in Fig. 1. Noteworthy is that period-doubling does not involve cusps but, as expected, a smooth doubling of the return map. Thus, generic bifurcation diagrams for the Mackey–Glass system are expected to display combinations of both isolated and doubling branches, with the birth/death of the former governed by Eq. (2), which is generic for delayed feedback systems. Note that while period-doubling implies a doubling in the number of peaks, in general peak-adding does not significantly alters the value of the period length. The frequently used term “period-adding” is a misnomer.

### 4. Impact of waveform deformations in phase diagrams

What is the impact of peak creation and destruction by waveform deformation in the overall organization observed in the control parameter space? It is overwhelming. This is illustrated by Fig. 4, which was obtained by following the same procedure as in Ref. [16], namely by counting the number of peaks (maxima) in a period of  $x(t)$  and codifying them in different tonalities, as indicated in the colorbar in the figure. As Fig. 4 shows, both the shape and the distribution of the several periodicity domains conjure to form a highly intricate mosaic that is quite difficult to be described by other means than graphical illustration. It is important to emphasize that all phase diagrams presented here display only stable phases, not boundaries of instability that cannot be measured experimentally.

Recall that a *single* delay-differential equation is already equivalent to an *infinite* dimensional set of ordinary first order differential equations [9–12]. This means that delayed feedback systems are far more complicated, general and richer than systems governed by ODEs. Thus, it is natural to expect DDEs to display all features which are familiarly found in ODEs. For instance, “shrimps” [17–24] were reported recently for a three-equations delayed feedback model intended to describe the dynamics of a red grouse population [25]. Similar shrimp-shaped domains of stability also exist abundantly in the Mackey–Glass equation as may be seen from

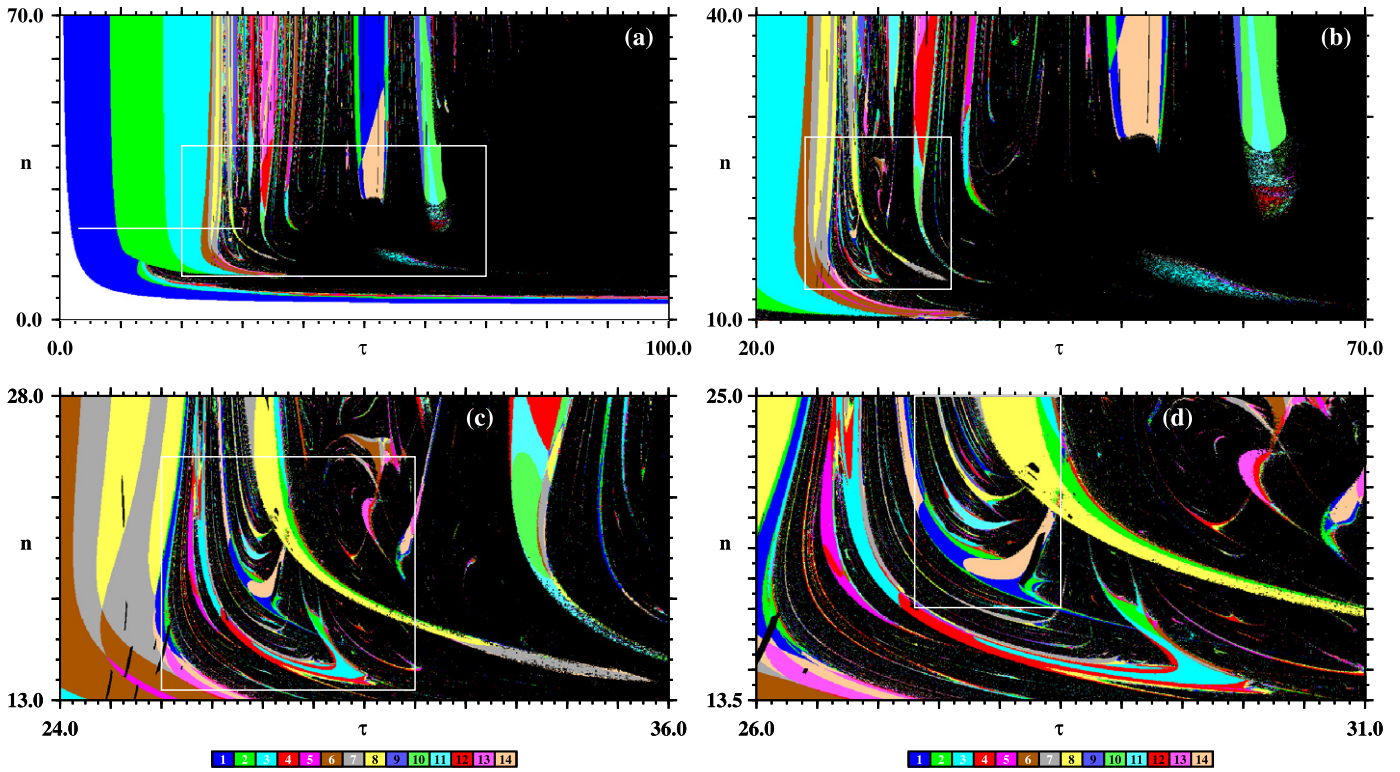


**Fig. 4.** (Color online.) Phase diagrams displaying an intricate mosaic of high periodicity regions, characterized individually by the number of peaks in a period of  $x(t)$ , as indicated by the colorbar. Chaotic phases are shown in black. (a) Global view of parameter space, with the  $n = 21$  horizontal line segment indicating the parameter interval considered in Figs. 1 and 2. The white domain in the lower-left corner denotes non-zero fixed points (non-oscillatory solutions). (b)–(d) Magnifications of the white boxes. The white box in (d) is enlarged in Fig. 5 below. Colors are used “mod 14”, i.e. we recycle the same colors for higher periods. Each panel displays the phase-space analysis of  $1000 \times 1000$  parameter points.

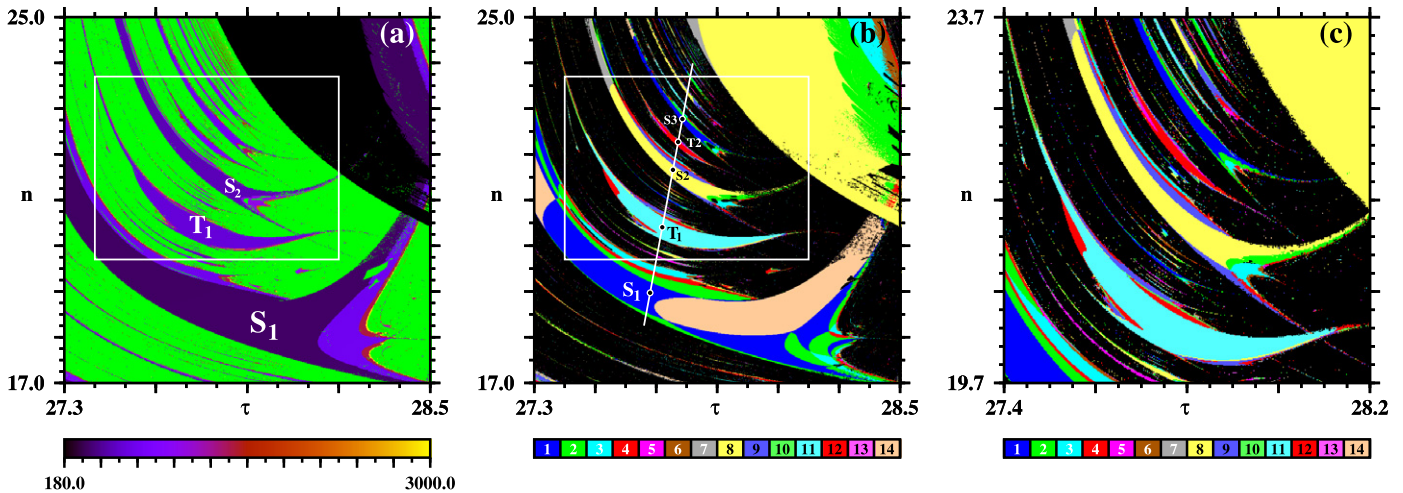


**Fig. 5.** (Color online.) The typical “chaos-periodicity alternations” observed between the new three-chaos-flanked periodicity islands  $T_i$  and the two-chaos-flanked shrimps  $S_i$  [17,18]. (a) Distribution of the period length inside the periodicity islands. Here, chaos is shown in green. (b) Same region as in (a), plotted now as an “isospike diagram” [16], obtained by counting the number of peaks within a period of the solutions. Identical colors indicate identity in the number of peaks in a period. The profusion of colors illustrate the mosaic formed by the infinite alternation of islands of periodicity. Chaos is shown in black. (c) Enlargement of the white box in (a) and (b). Individual panels display  $600 \times 600$  parameter points.

the white box in Fig. 4(d), shown magnified in Fig. 5. However the key questions are: what features can we observe in DDEs that are not known for ODEs? Are there many?

The control parameter space of delayed feedback systems displays a large number of novel features characteristic of their much higher-level of complexity. For example, the familiar shrimp-shaped domains mentioned above contain a much richer inner distribution of oscillatory patterns, as reflected by the profusion of colors of the intricate mosaic of periodicity windows in Fig. 4. Gen-

eralized routes to chaos which mix together period-doubling and peak-adding phenomena [26–29] are present profusely in DDEs.

Another surprising feature is easily recognizable from the white domain in the lower-left corner in Fig. 4(a): the effective impact in the system of a sudden increase from low to infinite dimensionality during the passage from  $\tau = 0$  to  $\tau \neq 0$ . As it is known, the delays underlying feedback systems require continuous sets of initial conditions in order to integrate them, being therefore embedded in an infinite-dimensional phase-space. An important question

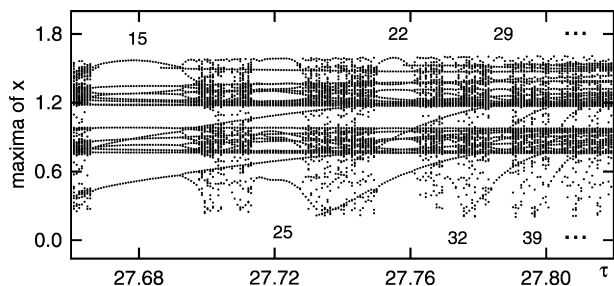


**Fig. 6.** Bifurcation diagram showing the periodicity windows  $S_i$  (upper labels) and  $T_i$  (lower labels) separated by windows of chaos. This diagrams was obtained by varying two parameters simultaneously along the white line, Eq. (3), seen in Fig. 5(b). Representative parameters for the main periodicity windows are given in Table 1.

**Table 1**  
Coordinates and number of peaks of the structures  $S_i$  and  $T_i$  seen in Fig. 5.

Structure	$\tau$	$n$	# of peaks $N_i$
$S_1$	27.6800	18.9710	15
$T_1$	27.7200	20.4050	25
$S_2$	27.7550	21.6600	22
$T_2$	27.7720	22.2700	32
$S_3$	27.7860	22.7720	29
$T_3$	27.7945	23.0760	39
$S_4$	27.8020	23.3460	36
$T_4$	27.8068	23.5180	46

whose answer is still lacking is the one about the impact of the sudden “explosion” of the number of degrees of freedom when delays are switched on in finite-dimensional systems. The wide non-zero fixed-point domain lying below the hyperbola forming the lower-left boundary in Fig. 4(a) gives clear evidence of the relative “lethargy” of the system to react to the passage from one to infinite degrees of freedom. First, as shown in Fig. 4(a), up to quite high values of  $n$  the onset of higher dimensionality does not alter the prevailing dynamics *instantaneously*. Would it be possible to characterize lethargy analytically, particularly when involving just simple fixed-points? Second, even more surprising is the fact that for low values of  $n$  the passage from one to infinite degrees of freedom has no effect at all in the dynamics, no matter how big the delay might be. Can such lack of influence be anticipated analytically, in general?

After characterizing in Fig. 4 the global impact of the waveform deformations seen in Fig. 1, we now show in Fig. 5 a remarkable new class of periodicity windows that we observed in DDEs and that, as far as we know, were not seen before, neither in ODEs nor in maps. As it is known, shrimps contain two flanks along which period doubling cascades occur [17–24]. However, as illustrated in Fig. 5, periodic oscillations for DDEs may also emerge forming periodicity islands with a very peculiar topological shape, characterized by three flanks along which period-doubling cascades and chaos occur. The largest of such islands are indicated by the labels  $T_i$  in Fig. 5 while shrimps are indicated by  $S_i$ . As shown in this figure, DDEs not only present three-chaos-flanked periodicity domains  $T_i$ , but the domains  $T_i$  and  $S_i$  emerge in sequences that alternate infinitely, increasing their periods and their number of peaks as  $n$  increases, forming unexpected routes to chaos which accumulate towards specific and wide regions of periodicity.

**5. Coding of oscillatory patterns**

From the regularities in Fig. 5 one may wonder what sort of modifications  $x(t)$  undergoes in order to produce the alternation of the  $S_i$  and  $T_i$  structures as the number of peaks in  $x(t)$  grow and the structures accumulate upwards in the figure. The aim of

this section is to show that the waveforms characterizing such alternation can be encoded in a relatively simple way, using a small number of minimal sub-patterns composing the waveforms.

To this end, we investigate the nature of the dynamical changes when crossing the  $S_i$  and  $T_i$  structures along some representative line, say, along the white line in Fig. 5(b) whose equation, for  $\tau$  in the interval  $27.66 \lesssim \tau \lesssim 27.82$ , is

$$n = 35.86\tau - 973.634. \tag{3}$$

More specifically, we computed a bifurcation diagram along this line, shown in Fig. 6. This diagram displays a rather complex alternation of windows of chaos and periodicity from which it is not possible to discern  $S_i$  from  $T_i$ . For some representative points along the white line, Eq. (3), we determined the number of peaks in each period. The number of peaks are given both in Fig. 6 and, along with their coordinates, in Table 1. From the table it is obvious that the number  $N_i$  of peaks in both  $S_i$  from  $T_i$  obeys a simple relation, namely

$$N_{i+1} = N_i + 7, \tag{4}$$

and that, in addition,  $T_i$  contains 10 peaks more than  $S_i$ .

To see how these extras peaks progressively change the waveform when parameters vary, Fig. 7 compares solutions  $x(t)$  for the parameters listed in Table 1. The left column in Fig. 7 shows the evolution of  $x(t)$  for the  $S_i$  structures while on the right column we show the evolution for the  $T_i$ .

From the waveform for  $S_1$  plotted in the top-left panel it is not difficult to recognize that  $x(t)$  may be subdivided according to the internal distribution of peaks in the pattern. Thus,  $S_1$  is composed by (i) two segments each containing three peaks, shown against a bluish background, (ii) a segment containing five peaks plotted against a beige and, finally, (iii) a four peaks segment plotted against a green background. Although the two segments containing three peaks look quite similar, they are not identical. However, for simplicity we focus here in the number of peaks, not on exact identity of patterns.

The subdivision of waveform  $x(t)$  for  $S_1$  into colored segments may be further simplified associating a letter  $A, B$ , etc. to each color. Thus, the internal subdivision of  $x(t)$  for  $S_1$  may be represented by the string  $ABAC$ . Now, looking at  $S_2$  in Fig. 7 one realizes that it may be also decomposed as above: in addition to the  $A, B, C$  segments in common to  $S_1$ , the waveform contains a new four-peaked segment that we paint yellow and denote by  $D$ . The whole pattern may be abbreviated  $ABADAC$ , where the underlined letters represent the 3 + 4 extra peaks that the waveform acquires when passing from  $S_1$  to  $S_2$ . The waveform of the  $T_i$  structures may be decomposed in a similar way. Table 2 summarizes the quite regular waveform subdivision as the period grows, with the letters inside the boxes indicating the position where the new 7 peaks are added when passing from  $i$  to  $i + 1$ . We stress the fact that letters are used here to summarize identity in the number of peaks but just similarity [not identity] of the waveform segment corresponding to them. In other words, letters are not meant to imply that subdivision remain invariant and/or are perfectly identical. In particular, from Fig. 7 one may spot differences between patterns corresponding to the same letter as  $i$  grows.

It is interesting to observe that the deformations of the segments corresponding to the various letters  $A, B, C, E$  change very little when passing from one shrimp  $S_i$  to the next, or from one  $T_i$  to the next. But this is not true for segment  $D$  whose shape evolves sensibly more. Comparing the leftmost with the rightmost  $D$  segments in  $T_4$  it is possible to recognize that they are not identical and are looking more and more like  $C$ . It is remarkable that when  $i$  grows the waveforms for  $S_i$  and  $T_i$  increase by the invariant pattern  $AD$  which is “inserted” always in the same position, to

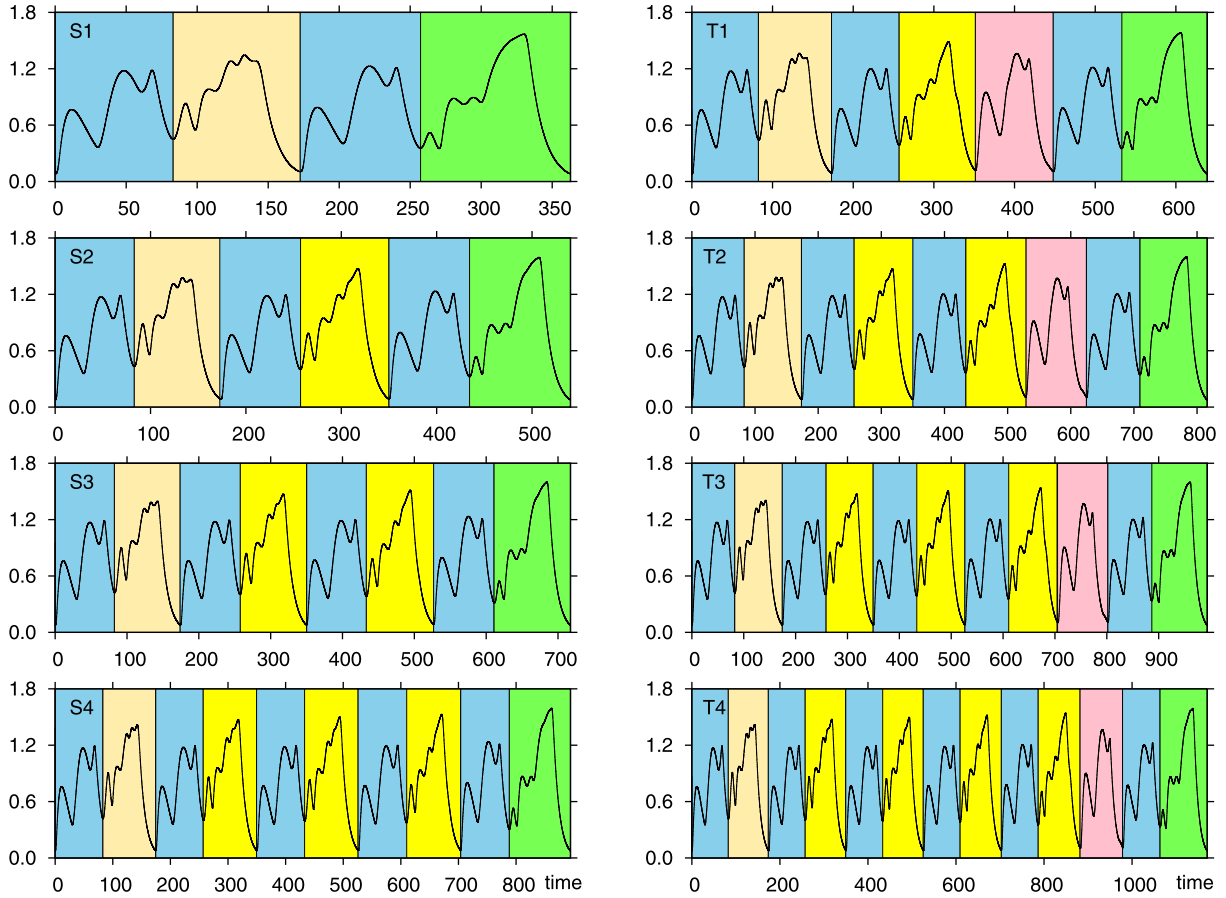


**Fig. 7.** (Color online.) Temporal evolution of  $x(t)$  computed for representative parameters inside the periodic  $S_i$  and  $T_i$  structures located along the white line in Fig. 5(b), and defined in Table 1. All functions are periodic and can be decomposed in a small number of sub-patterns as indicated by the colors and encoded in regular strings of symbols (see text).

**Table 2**  
Subdivision of the waveforms  $S_i$  and  $T_i$  in Fig. 7. Boxes indicate position of new peaks which appear when passing from  $i$  to  $i + 1$ .

$i$	$S_i$	$T_i$
1	ABAC	ABADEAC
2	AB $\overline{AD}$ AC	ABAD $\overline{AD}$ EAC
3	ABAD $\overline{AD}$ AC	ABADAD $\overline{AD}$ EAC
4	ABADAD $\overline{AD}$ AC	ABADADAD $\overline{AD}$ EAC

the left of AC and EAC, respectively, as indicated in Table 2. The net effect of this insertion is to induce a shift of subdivisions to the left.

**6. Conclusions and outlook**

We reported a number of phenomena observed in phase diagrams obtained by systematic numerical investigation of a paradigmatic delayed feedback system, the Mackey–Glass DDE. Periodic solutions of this system were shown to display continuous deformations of their waveforms as control parameters are varied. Such deformations create and destroy peaks in the oscillatory patterns. Peak creation and destruction results in rich and intricate *isolated* branches appearing and disappearing in bifurcation cascades. As a result of the added flexibility of incorporating an odd number of branches, sequences of branching cascades in DDEs may emerge in rich combinations of the familiar peak-adding and period-doubling bifurcations, something that we believe not to have been observed in ODEs. Such branching cascades produce highly intricate mosaics

of periodicity domains in control parameter space, tiling it with very complicated patterns, both regular or not. Further, we found that the waveforms of families of oscillations can be described systematically in terms of a rather small number of sub-waveforms combined in rather simple way. We hope all the aforementioned novel features to motivate their experimental validation in the near future, particularly since the Mackey–Glass equation can be realized electronically in the laboratory [30,31].

Our detailed numerical phase diagrams open the possibility of assessing the quality and the predictive power of the numerous approximate analytical methods and applications developed over the years for delay-differential equations. While it is usual to invariably claim analytical estimates of all sorts to be valid for “small parameters” and/or “small delays”, it is equally usual not to define what exactly should be understood by the term small [32–34]. The computation of detailed numerical phase diagrams provides a stringent reference frame against which to check the validity of all such valuable approximations. They also challenge one to try to go beyond standard fixed-point analysis. An interesting open question is to investigate whether the powerful multiple scaling method efficiently applied to a DDE with a single control parameter [35] could be also effective for the three effective parameter Mackey–Glass equation. In particular, it would be interesting to investigate whether or not the metric properties found numerically in Ref. [35] for a system containing a single control parameter survive when several parameters are changed.

Finally, another characteristic feature of DDEs that we observed to hold over wide parameter ranges is that the onset of higher-dimensionality does not alter the prevailing dynamics

instantaneously, and even may have no effect at all. This remarkable “lethargic effect” cannot be obtained using the familiar perturbative techniques to define the stability of fixed-points or to estimate the boundaries where Hopf bifurcations occur [12]. Furthermore, lethargy is not a peculiarity of the Mackey–Glass equation but was also found in realistic and well-known lasers systems [8]. To us, the ubiquitous lethargy in the response seems to provide strong evidence that a nice result obtained by Mallet-Paret [33] for a certain type of delay-differential equations, showing the topological dimension of phase space to be effectively finite, may also apply to a much wider class of systems than originally thought. Something that of course needs further investigation.

### Acknowledgements

JACG is indebted to Prof. L. Glass and Prof. M.C. Mackey for helpful email exchanges and references. The authors thank Prof. Thorsten Pöschel for the kind invitation and hospitality at the Friedrich-Alexander Universität Erlangen–Nürnberg. This work was supported by the Deutsche Forschungsgemeinschaft through the Cluster of Excellence *Engineering of Advanced Materials*. LJ is supported by a CNPq Doctoral Fellowship. JACG is supported by CNPq and AFOSR, grant FA9550-07-1-0102. All bitmaps were computed in the CESUP-UFRGS clusters.

### References

- [1] M.C. Mackey, L. Glass, *Science* 197 (1977) 4300; M.C. Mackey, L. Glass, *Scholarpedia* 5 (3) (2010) 6908.
- [2] L. Glass, M.C. Mackey, *From Clocks to Chaos: The Rhythms of Life*, Princeton University Press, Princeton, 1988.
- [3] M.C. Mackey, *Case Studies in Mathematical Modeling – Ecology, Physiology and Cell Biology*, Prentice-Hall, New Jersey, 1997, Chapter 8.
- [4] J.-M. Liu, in: V. In, et al. (Eds.), *Understanding Complex Systems*, Springer, Berlin, 2009.
- [5] T. Erneux, P. Glorieux, *Laser Dynamics*, Cambridge University Press, Cambridge, 2010.
- [6] M.B. Hoagland, B. Dodson, J. Hauck, *The Way Life Works: The Science of Biology*, Jonea and Bartlett, Sudbury, 2001.
- [7] K.J. Astrom, R.M. Murray, *Feedback Systems, An Introduction for Scientists and Engineers*, Princeton University Press, Princeton, 2008.
- [8] L. Junges, J.A.C. Gallas, 2012, submitted for publication.
- [9] H. Smith, *An Introduction to Delay-Differential Equations with Applications*, Springer, New York, 2011.
- [10] F.M. Atay (Ed.), *Complex Time-Delay Systems*, Springer, Berlin, 2010.
- [11] W. Just, A. Pelster, M. Schanz, E. Schöll (Eds.), *Delayed Complex Systems*, *Phil. Trans. R. Soc. A* 368 (2010) 301, Theme issue.
- [12] T. Erneux, *Applied Delay Differential Equations*, Springer, NY, 2009.
- [13] J. Wei, *Nonlinearity* 20 (2007) 2483.
- [14] A. Wan, J. Wei, *Nonlin. Dyn.* 57 (2009) 85.
- [15] M.A. de Menezes, R.M.Z. dos Santos, *Int. J. Mod. Phys. C* 11 (2000) 8.
- [16] J.G. Freire, J.A.C. Gallas, *Phys. Chem. Chem. Phys.* 13 (2011) 12191; J.G. Freire, J.A.C. Gallas, *Phys. Lett. A* 375 (2011) 1097.
- [17] Shrimps are formed by a regular set of adjacent windows centered around a main pair of parabolic arcs. A shrimp is a *doubly infinite mosaic* of stability domains composed by an innermost *main* domain plus all the adjacent periodicity domains arising from two period-doubling cascades together with their corresponding domains of chaos [18]. Shrimps should not be confused with their innermost main domain of periodicity or with superstable loci characteristic of one-dimensional maps. For details see Ref. [18].
- [18] J.A.C. Gallas, *Phys. Rev. Lett.* 70 (1993) 2714; J.A.C. Gallas, *Physica A* 202 (1994) 196; J.A.C. Gallas, *Appl. Phys. B* 60 (1995) S203; B.R. Hunt, J.A.C. Gallas, C. Grebogi, J.A. Yorke, H. Koçak, *Physica D* 129 (1999) 35; For recent developments see Refs. [20–24].
- [19] E.N. Lorenz, *Physica D* 237 (2008) 1689.
- [20] Y.C. Lai, T. Tél, *Transient Chaos*, Springer, New York, 2011.
- [21] J. Argyris, G. Faust, M. Haase, R. Friedrich, *Die Erforschung des Chaos*, Zweite Auflage, Springer, Berlin, 2010.
- [22] For a survey see J.A.C. Gallas, *Int. J. Bif. Chaos* 20 (2010) 197, and references therein.
- [23] R. Vitolo, P. Glendinning, J.A.C. Gallas, *Phys. Rev. E* 84 (2011) 016216.
- [24] R. Barrio, F. Blesa, S. Serrano, A. Shilnikov, *Phys. Rev. E* 84 (2011) 035201(R).
- [25] J. Slipantchuk, E. Ullner, M.S. Baptista, M. Zeineddine, M. Thiel, *Chaos* 20 (2010) 045117.
- [26] M. Levi, *SIAM J. Appl. Math.* 50 (1990) 943.
- [27] C. Bonatto, J.C. Garreau, J.A.C. Gallas, *Phys. Rev. Lett.* 95 (2005) 143905; C. Bonatto, J.A.C. Gallas, *Phys. Rev. E* 75 (2007) 055204(R); C. Bonatto, J.A.C. Gallas, *Phil. Trans. R. Soc. London A* 366 (2008) 505; V. Kovanis, A. Gavrielides, J.A.C. Gallas, *Eur. Phys. J. D* 58 (2010) 181; J. Bragard, et al., *Phys. Rev. E* 84 (2011) 037202, see also Ref. [16].
- [28] R.E. Francke, T. Pöschel, J.A.C. Gallas, in: *Studies in Computational Intelligence*, Springer, Berlin, 2012.
- [29] A. Sack, T. Pöschel, E. Lindberg, J.A.C. Gallas, *Discontinuous spirals of periodicity and chaos in a noiseless Duffing proxy: Theory and experiments*, 2012, submitted for publication.
- [30] A. Namajunas, K. Pyragas, A. Tamasevicius, *Phys. Lett. A* 201 (1995) 42.
- [31] S. Sano, A. Uchida, S. Yoshimori, R. Roy, *Phys. Rev. E* 75 (2007) 016207.
- [32] R.E. O'Malley Jr., *SIAM Rev.* 13 (1971) 425.
- [33] J. Mallet-Paret, *J. Diff. Eqs.* 22 (1976) 331.
- [34] C. Chicone, *J. Diff. Eqs.* 190 (2003) 364.
- [35] M. Schanz, A. Pelster, *Phys. Rev. E* 67 (2003) 056205.